https://ntrs.nasa.gov/search.jsp?R=19700019509 2018-07-24T00:24:13+00:00Z

U. of Iowa 70:17

N 70 28819

NASA CR 110013

CONJUGATE PHOTOELECTRON IMPACT IONIZATION*

S. D. Shawhan, L. P. Block,**
and C.-G. Falthammar**

CASE FILE COPY

Department of Physics and Astronomy
THE UNIVERSITY OF IOWA
Iowa City, Iowa

U. of Iowa 70-17

CONJUGATE PHOTOELECTRON IMPACT IONIZATION*

S. D. Shawhan, L. P. Block,**
and C.-G. Falthammar**

Department of Physics and Astronomy
The University of Iowa
Iowa City, Iowa 52240

March 1970

*Work supported at The University of Iowa under NASA grants NGL-001-002 and NGR-16-001-043.

**Division of Plasma Physics, Royal Institute of Technology, 10044 Stockholm, Sweden.

ABSTRACT

The exchange of photoelectrons between ionospheres in a matter of minutes rather than at the slow ambipolar speed is discussed. It is shown that the electron density may be affected by secondary processes resulting from the conjugate photoelectron flux but not by the flux itself.

The flux spectrum of conjugate photoelectrons throughout the day at the solstices for minimum solar activity is calculated for 55°N. geographic latitude over Europe, using a method previously employed by NISBET. Summer escaping flux values range up to 9×10^{12} electrons m^{-2} sec^{-1} and winter values to 5×10^{12} electrons m^{-2} sec^{-1}. Compared at specific solar zenith angles the computed values are in good agreement with recent satellite measurements. Approximately half of this flux is lost by Coulomb collisions along the field line path. The resulting flux arriving at the local ionosphere produces ionization by inelastic collisions in the atmosphere. This additional ionization is about 3% of the ionization from local processes at summer noon and 48% at winter noon. During winter nighttime this conjugate photoelectron ionization can be signficant for several hours.

Although small in magnitude, this additional ionization should systematically modify the summer total electron content depending on geographic location. The large seasonal differences in the relative impact ionization may explain in part the F-layer seasonal anomaly. This source may be important for maintaining and causing enhancements in the winter nighttime ionosphere.

1. INTRODUCTION

The exchange of photoelectrons between magnetically conjugate parts of the ionosphere has been successfully invoked in explaining F-layer electron heating (e.g. HANSON, 1963; CARLSON, 1966; EVANS, 1968; NISBET, 1968; and NAGY, et al., 1969). Such exchange should also influence the electron density itself (the profile as well as the total content). This possibility has not attracted much attention so far although LISZKA (1967) conjectured that this exchange may explain the forenoon peaks observed in the summer (solar minimum) total electron content at high latitudes.

In Section 2 several mechanisms for the exchange of photoelectrons are discussed. It is concluded that the photoelectron flux itself does not affect the electron density but that the secondary effects of heating, excitation and impact ionization may be important (Section 3). In this paper we discuss a model calculation to determine the additional ionization rate due to impact ionization by photoelectrons from the conjugate ionosphere.

The numerical computations proceed by first obtaining a photoelectron production rate energy spectrum in a multicomponent atmosphere at different local times and altitudes for solar minimum

summer and winter (Section 4). Using the method of NISBET (1968) the photoelectron escaping flux energy spectrum is obtained (Section 5); elastic and inelastic collisions with neutrals and Coulomb collisions with thermal electrons are included. Assuming only Coulomb collisions along the field line path (above 600 km) between the magnetically conjugate ionopsheres, the arriving photoelectron flux energy spectrum is evaluated (Section 6). In Section 7 the resulting impact ionization is calculated and found to be significant compared to the ionization from entirely local processes. Some possible improvements on the computational model are discussed in Section 8. Finally, several expected consequences of this additional impact ionization on the diurnal variation of the electron density profile and of the total electron content are pointed out (Section 9).

2. PHOTOELECTRON DIFFUSION MECHANISM

Satellite observations of photoelectron fluxes (e.g. GALPERIN and MULYARCHIK, 1967, and RAO and DONNLEY, 1969) and observations of increases in electron temperature before local sunrise (e.g. CARLSON, 1966) and optical line emissions in twilight (e.g. BROADFOOT and HUNTEN, 1966) indicate that photoelectrons escape from the ionosphere and travel between conjugate regions of the ionosphere in a matter of minutes. In order to properly interpret the effects of these conjugate photoelectrons the photoelectron diffusion mechanism must be understood.

Since quasineutrality is valid throughout the regions concerned, an increase of electron density anywhere due to the influx of photoelectrons must be accompanied by a corresponding increase of ion density. Otherwise, the conjugate ionosphere would become charged in such a way that the photoelectron flux would be stopped by a retarding potential which is apparently not observed. The ambipolar diffusion process by which ions and electrons diffuse together along field lines between conjugate ionospheres has been studied theoretically by KOHL (1966) and CUMMACK (1968). They find, however, that the diffusion time from one hemisphere to the other

is several hours, and that the flux is probably too low to be of any great importance. In fact, because of the long diffusion time any magnetospheric convection will cause a large displacement of the diffusing particles from the initial magnetic flux tube.

There are two other ways in which quasineutrality can be maintained. First, there may be an ionic Pedersen current in the lower ionosphere. The magnitude of this current would correspond to an ion flux which is equal to the conjugate photoelectron flux; the ions would diffuse across field lines at low altitudes and electrons would travel along the field line from the conjugate point. Then photoelectrons can travel between conjugate ionospheres in a few minutes rather than at the slow ambipolar speed, and the flux itself gives a net contribution to the electron density at the receiving ionosphere.

The second way of preserving quasineutrality is by a return diffusion flux of thermal electrons (many more at lower velocity) along the same magnetic field line (cf. RISHBETH, 1968). This exchange leads to a redistribution of electron energies between conjugate ionospheres, but no net displacement of ionization occurs so that the electron density is not changed directly by this flux. In both cases the photoelectrons can also cause impact ionization, excitation, and heating. Of these two mechanisms, the process requiring the lowest driving potential will dominate. This potential must also be small compared with typical conjugate photoelectron energies if the conjugate photoelectron flux is not to be inhibited.

A Pedersen current requires a voltage of the order of

$$V_p = \frac{e\varphi l_1 l_2}{\Sigma_p l_1/L} = e\varphi l_2 L/\Sigma_p \qquad (1)$$

where e = elementary charge

φ = conjugate photoelectron flux per unit area

l_1 = longitudinal extent of conjugate photoelectron flux

l_2 = latitudinal extent of conjugate photoelectron flux

L = effective distance in the ionosphere between the conjugate points

Σ_p = height integrated Pedersen conductivity

With $\varphi = 10^{12}$ electrons/m^2 sec, $L = 10^4$ km and $\Sigma_p = 0.5$ ohm^{-1} (BOSTRÖM, 1964) we get

$$V_p \text{ (volts)} \approx 3 l_2 \text{ (meters)} \qquad (2)$$

Since l_2 is at least of the order of a hundred kilometers, V_p would have to be of the order of 10^5 volts or more in order to drive an ion flux in the low ionosphere comparable to the photoelectron flux along the geomagnetic field lines. Hence, this mechanism cannot possibly operate.

The potential necessary to drive a return flux of thermal electrons along the magnetic field line is

$$V_{\parallel} = e\varphi L_{\parallel}/\sigma_{\parallel} \approx 0.5 \text{ volts} \tag{3}$$

where $L_{\parallel} = 10^5$ km is the length of the geomagnetic field line and $\sigma_{\parallel} = 30$ ohm^{-1} m^{-1} (BOSTRÖM, 1964). Consequently, only a small potential will cause a neutralizing return flux of thermal electrons. This mechanism of exchange between photoelectron and thermal electron fluxes seems the most likely to operate.

In discussing the time scales of the exchange mechanism, the concept of a two-component electron gas, consisting of thermal electrons and photoelectrons can be used. The photoelectrons have energies from a few eV to more than 60 eV. For such a model, one can use generalized ambipolar-diffusion equations to calculate the time scales of the exchange. The ambipolar electric field (which depends on a combination of diffusion coefficients, mobilities and densities of the two electron components) is weak enough to influence the photoelectrons only a little but the thermal electrons very much. The end result is that the photoelectrons are nearly unaffected by the quasineutrality constraint. Therefore, the characteristic time for their exchange between conjugate ionospheres is of the order of minutes only. The diffusion of the thermal electron population consists of two parts. One has a flux which is precisely equal and opposite to the photoelectron diffusion flux, and the other is coupled with the mobility of the ions and has essentially the ordinary ambipolar character with the correspondingly long time scale.

3. SECONDARY PROCESSES AFFECTING THE ELECTRON DENSITY

The conjugate photoelectrons do not contribute to the electron density directly because their flux is precisely cancelled by a return flux of thermal electrons. However, this photoelectron flux causes secondary processes which can change the electron density: heating, impact ionization and excitation. The heating influences the loss processes. The dissociative recombination coefficient appropriate for low altitudes seems to decrease with temperature (see SWIDER, 1965), whereas the ion-atom interchange coefficient appropriate for high altitudes increases with electron temperature (see THOMAS, 1968). Most of the loss occurs at low altitudes where the heating is small and is likely to be unimportant. As better data on the loss rate coefficients and on the atmospheric parameters become available this heating effect should be checked quantitatively.

Impact ionization represents an addition to the local photoionization and impact ionization from locally produced photoelectrons. The magnitude of this additional source is calculated in the following sections and compared to the local sources.

Excitation processes are important for explaining the optical emissions. They are also important in calculating the conjugate photoelectron impact ionization because the excitation processes compete with the impact ionization processes.

4. PHOTOELECTRON PRODUCTION SPECTRUM

In order to evaluate the magnitude of impact ionization by photoelectrons from the conjugate ionosphere and the diurnal, the seasonal and the altitudinal variations of this magnitude, model calculations have been carried out. Calculations are made between local sunrise and sunset for solar minimum summer and winter. A geographic location of 55° N latitude over Europe is assumed giving a geomagnetic latitude of 52° and a conjugate point at 46° S geographic latitude.

The photoelectron production rate spectrum calculation follows that of TOHMATSU (1965). The production rate at 20 km intervals between 100 km and 600 km is calculated for each ionic species by the relation

$$q(X,\lambda,h,\chi) = \sigma_{ion}(X,\lambda)n(X,h)F_o(\lambda)\exp[-\tau(\lambda,h,\chi)] \qquad (4)$$

where τ is the optical depth given by

$$\tau(\lambda,h,\chi) = \sum_X \sigma_{abs}(X,\lambda)\int n(X,h)ds \qquad (5)$$

where σ_{ion} is the photoionization cross-section and σ_{abs} the photo-absorption cross-section for species X at wavelength λ. F_o is the photon flux at the top of the ionosphere at wavelength λ. These quantities are taken from HINTEREGGER, et al. (1965) for species O, O_2, N_2 and a wavelength range of 665 Å to 150 Å. Diurnal neutral atmosphere models n(X) are taken from HARRIS and PRIESTER (1962) for solar minimum (S = 70 model). It is assumed that these models apply at the latitudes of interest during both summer and winter. The integral in equation (5) is replaced by the following approximation:

$$\int n(X,h)ds = n(X,h)H(X,h) \sec \chi \qquad (6)$$

where H is the scale height for specie X at altitude h given in the atmosphere models and χ is the solar zenith angle which depends on the season and local time.

Equation (4) then gives the production rate at a given solar zenith angle and altitude for a given species and wavelength. The photoelectron production rate spectrum is obtained by multiplying this production rate by the probability of ionization to a certain electronic state for a given species and wavelength. This resulting production rate is added to the rate in the particular 2 eV interval from 0 to 100 eV which brackets the value of the excess energy transferred to the photoelectrons. Values for the ionization probabilities and excess energy transferred to the photoelectrons are taken from TOHMATSU, et al. (1965).

Examples of the height integrated (100 km - 600 km) primary photoelectron production rate spectra up to 80 eV are shown for summer and winter noon at the conjugate ionosphere in Figure 1. Note that these curves exhibit a characteristic maximum between 40 eV and 60 eV and that the spectrum falls off sharply above 60 eV. Consequently, photoelectron energies up to 62 eV are considered in further calculations.

Electrons are also produced from impact ionization by the primary photoelectrons. This secondary spectrum is obtained as a result of the calculation in the next section. In general, these secondary photoelectrons are at low energies and increase the total photoelectron production (summed over altitude and energy) by at most 10%.

5. ESCAPING PHOTOELECTRON FLUXES

In order to obtain the photoelectron flux spectrum escaping the conjugate ionosphere from the photoelectron production rate spectrum, the method employed by NISBET (1968) is used.

For each 2 eV photoelectron energy interval centered on 1 eV to 61 eV and for each altitude (20 km intervals, 100 km to 600 km) the continuity equation is solved for the photoelectron number density:

$$N_E = \frac{Q_E + G_E^{ie} + G_E^{e} - \mathrm{div}(N_E \bar{v})}{L_E^{ie} + L_E^{e} + F_E^{e}} \tag{7}$$

where

Q_E = the primary photoelectron production rate for a given altitude at energy E

$$G_E^{ie} = \sum_X \sum_W N_{E+W}\, v_{E+W}\, \sigma_{E+W}^{ie}\, n(X) \tag{8}$$

the gain of photoelectrons at energy E from higher energies due to inelastic collisions with neutral particles. This term includes the secondary ionization due to primary photoelectron impact.

$$G_E^e = 1.16 \times 10^{-10}\, n_e (E + 2)^{-1/2}\, N_{E+2} \qquad (9)$$

the gain of photoelectrons at energy E from the next higher energy interval E + 2 due to elastic (Coulomb) scattering with the ambient thermal electrons (BUTLER and BUCKINGHAM, 1962).

$$\mathrm{div}(N_E\, \bar{v}) = \mathrm{div}(\Phi_E^d) = \text{the gain or loss of photoelectrons} \qquad (10)$$

at energy E due to diffusion in altitude.

$$L_E^{ie} = \sum_X \sum_W v_E\, \sigma_{E-W}^{ie}\, n(X) \qquad (11)$$

the loss probability of photoelectrons to lower energies due to inelastic collisions with neutral particles.

$$L_E^e = 1.16 \times 10^{-10}\, n_e\, E^{-1/2} \qquad (12)$$

the loss probability of photoelectrons to the next lower energy level E - 2 due to elastic (Coulomb) collisions with ambient thermal electrons (BUTLER and BUCKINGHAM, 1962).

$$F_E^e = \sum_X v_E\, \bar{R}_E\, \sigma_E^e\, n(X) \qquad (13)$$

the probability of photoelectrons to make one elastic collision with neutral particles and then escape from the ionosphere without further collisions. This probability multiplied by the photoelectron number density and summed over all altitudes gives the photoelectron escape flux spectrum.

N_E is the photoelectron number density in the 2 eV interval centered on energy E (eV) for a given altitude. The photoelectron velocity is v_E . Values for the inelastic collision cross sections σ_E^{ie} (excitation and ionization) for energy E were scaled from the curves compiled by NISBET (1968). The ionization cross sections were extrapolated to 62 eV using the formula of LOTZ (1968). Diurnal electron density profiles n_e were obtained from the data of WATKINS and TAYLOR (1969). The time scales were expanded or contracted so that the ground sunrise and sunset times would be those at the local or conjugate location for summer (using April 1964 data) and winter (using October 1964 data).

Assuming that the photoelectron pitch angle distribution is isotropic over the upward hemisphere, the diffusion flux in the vertical direction is given by (NISBET, 1968).

$$\Phi_E^d = -\frac{1}{6}\lambda_E v_E \frac{dN_E}{dh} \sin^2 I \qquad (14)$$

where λ_E is the mean free path for a photoelectron of energy E and I is the magnetic dip angle. The probability that a given elastic collision will result in escape from the ionosphere without further collisions is given by $\bar{R}_E$. It is evaluated by NISBET (1968) assuming again an isotropic photoelectron distribution. Elastic collision cross sections σ_E^e are scaled from the curves in MCDANIEL (1964).

As equation (7) stands, it represents a matrix of equations coupled in energy and altitude. With the initial approximation of $\mathrm{div}(\Phi_E^d) = 0$ for all energies and altitudes the equations are uncoupled in altitude. The solution procedure is to assume that $N_E = 0$ for the highest energy (63 eV) . Then the equations can be solved for successively lower energies at any given altitude. Having the first approximation to $N_E(h)$ the divergence terms can be evaluated using equation (14). It is found for the assumed models that the divergence terms do not modify the resulting photoelectron escape flux by more than 10% and only at low energies for any local time so the divergence terms are neglected.

The method of NISBET (1968) is used to calculate the escaping photoelectron flux spectrum. The total photoelectron flux escaping from the ionosphere is composed therefore, of two terms. The first is the flux of photoelectrons which make an elastic collision and then escape without making another collision. This escape flux is obtained from equation (13)

$$\Phi_E^e = \int^{600\ \mathrm{km}} N_E\, F_E^e\, dh. \tag{15}$$

The second term is the diffusion flux given by equation (14) at an altitude for which the mean free path of the photoelectrons exceeds the scale height of the photoelectron distribution. In this case the diffusing particles are free to escape along the field line.

Examples of the total escaping photoelectron flux spectrum for summer and winter local noon at 600 km altitude are given by the solid curves in Figure 2. Note the maximum between 40 eV and 60 eV as a consequence of the maximum in the production spectrum. Also, the relative content of high energy electrons is slightly larger in summer. These spectra were calculated for different local times during the conjugate summer and winter daytime. The escaping photoelectron flux, integrated over all energies, at 600 km altitude is plotted against local time in Figure 3. Around summer noon the flux reaches 9×10^{12} electrons m^{-2} sec^{-1} whereas at winter noon it is 5.3×10^{12} electrons m^{-2} sec^{-1}.

The total photoelectron production (primary plus secondary) in the summer noon ionosphere is nearly three times the production in the winter noon ionosphere (3.6×10^{13} vs 1.4×10^{13} electrons m^{-2} sec^{-1}). However, the escape probability for these electrons is 38% in the winter and only 25% in the summer so that the escaping fluxes are within a factor of two as shown in Figure 3.

In Figure 4, the calculated values of the escaping flux for solar zenith angles χ of 80° to 110° are compared with satellite measurements of RAO and DONLEY (1969) with good agreement. At two solar zenith angles (86.4° and 91.2°) the calculated flux values for both sunrise and sunset are shown. As expected because of the lower electron content, the sunrise fluxes are higher. The comparison to experimental values is made for summer and winter for the flux

at 600 km and energies $E > 5$ eV. For the value of 2.5×10^{12} electrons m^{-2} sec^{-1} RAO and DONLEY (1969) reported in local winter daytime [χ(winter) = 57°, χ(summer) = 86°] the calculated flux would be 1.4×10^{12} electrons m^{-2} sec^{-1} escaping upward from the winter hemisphere and 4.1×10^{12} electrons m^{-2} sec^{-1} from the conjugate summer ionosphere. Also, the portion of the escaping flux that falls above 40 eV is within the range observed by COSMOS - 5 (GALPERIN and MULYARCHIK, 1967). These theoretical escaping flux values, therefore, seem to be in good agreement with experimental measurements.

6. ARRIVING PHOTOELECTRON FLUXES

Along the path from one ionosphere to the other above 600 km altitude, the escaping photoelectrons are assumed to suffer only Coulomb collisions with the thermal electrons. NISBET (1968) has performed extensive calculations which show that these collisions tend to keep the pitch angle distribution isotropic. These collisions also thermalize the low energy end of the initial escaping flux spectrum and slightly de-energize the higher energy photoelectrons.

Using the formula of BUTLER and BUCKINGHAM (1962) for energy loss by Coulomb collisions with thermal electrons , a photoelectron with initial energy E at the conjugate ionosphere will have an energy E' at the top of the local ionosphere

$$E' = [E^2 - \frac{3.9 \times 10^{-16}}{\cos \alpha} \int_{600\ \mathrm{km\ S}}^{600\ \mathrm{km\ N}} n_e \, d\ell]^{1/2} . \qquad (16)$$

For an isotropic distribution $\overline{\cos \alpha} = 0.5$ and for a total electron content of 1.3×10^{17} electrons m^{-2}

$$E'(eV) = [E^2(eV)^2 - 100(eV)^2]^{1/2} . \qquad (17)$$

Equation (17) indicates that photoelectrons with initial energies less than 10 eV will be de-energized to thermal energies and higher energy particles will loose some energy.

The resultant spectra for the arriving flux at noon in the winter and summer ionospheres are given by the dots and squares, respectively, in Figure 2. Note that the low energy portions of the spectra are modified significantly. The high energy portions are nearly the same as for the escaping flux at the conjugate ionosphere. Also, the spectrum arriving in the local winter is slightly "harder" (falls off less steeply) than the arriving summer spectrum.

In Figure 3, the arriving winter and summer fluxes are shown as a function of conjugate time by the short dashed and the dotted curves, respectively. Comparing the arriving winter to the escaping summer flux, 40% to 73% during the daytime was not thermalized along the path. During the daytime, 46% to 66% of the escaping winter flux was not thermalized.

7. CONJUGATE PHOTOELECTRON IMPACT IONIZATION

Arriving photoelectron flux spectra similar to those shown in Figure 2 have been calculated for other times during the conjugate daytime. Based on the conclusion of NISBET (1968) about the effect of scattering on the flux angular distribution, it is assumed that the arriving flux has an angular distribution such that the average velocity in the downward direction is $v_E/2$. The photoelectrons are thermalized by the competing processes of impact ionization, heating, and excitation.

The flux spectrum F_E for 20 km steps in altitude, starting at 600 km, is obtained from the set of linear differential equations

$$\frac{dF_E}{dh} = \sum_X \sum_W 2\, F_{E+W}\, \sigma^{ie}_{E+W}\, n(X) + 3.9 \times 10^{-18}\, n_e (E+2)^{-1}\, F_{E+2}$$

$$- \sum_X \sum_W 2\, F_E\, \sigma^{ie}_{E-W}\, n(X) - 3.9 \times 10^{-18}\, n_e E^{-1}\, F_E \qquad (18)$$

where the other quantities have the same meaning as in Section 5. At each altitude, the impact ionization is obtained from the relation.

$$Q_E^i = \sum_X 2\ F_E\ \sigma_E^{ion}\ n(X)\ , \tag{19}$$

where σ_E^{ion} is the impact ionization cross section for a given species.

Representative impact ionization rate profiles due to conjugate photoelectrons are shown in Figure 5 for local summer and winter noons. For comparison, the photo plus secondary photoelectron production rate profile as well as a loss rate probability (L/n_e where L is calculated using $\alpha = 3 \times 10^{-13}\ m^3\ sec^{-1}$, $\gamma(N_2) = 3 \times 10^{-19}\ m^3\ sec^{-1}$ and $\gamma(O_2) = 3 \times 10^{-18}\ m^3\ sec^{-1}$; SWIDER, 1965) are shown. The relative contribution of this ionization to the electron density depends not only on the relative magnitude of the conjugate photoelectron ionization rate but also on the altitude at which this ionization is created. Ionization produced at high altitude contributes more because it has a longer life-time.

As is seen from Figure 5, the maximum conjugate photoelectron impact ionization in summer occurs 30 km higher than the maximum total local ionization and both occur well above the maximum of the loss region (140 km). This impact ionization has a long life-time (of the order of several hours) which results in a larger contribution than its modest relative magnitude would indicate. At 230 km, the conjugate impact ionization is 4.7% of the total local ionization. During local winter, the peak of the additional ionization occurs approximately 40 km lower than the peak of the local ionization

but still well above the peak loss region. However, this additional ionization is equal to the local ionization at 220 km and is 26% at 320 km for the case of local noon.

In Figure 6 are plotted the height integrated impact ionization rate due to the conjugate photoelectrons for summer and winter local daytimes. The time of local sunrise (LSR) and sunset (LSS) as well as conjugate noon (CN) are indicated by the arrows. Because of the geographic location of the magnetic conjugate point, conjugate noon occurs at 10.2 hours local time for the model considered. On comparing these height integrated impact ionization curves to the arriving conjugate flux curves of Figure 3, the impact ionization efficiency can be computed. For local summer daytime, it ranges from 0.36 to 0.46 and for local winter daytime from 0.31 to 0.49, both averaging about 0.40.

For comparison, the height integrated photoionization rate plus the secondary ionization rate due to impact ionization by local photoelectrons is also plotted in Figure 6. During summer, the ionization due to conjugate photoelectrons is a small fraction (3.2% at local noon). Most importantly, during winter nighttime, particularly before sunrise, when the local photoproduction vanishes, the conjugate photoelectron impact ionization is quite significant for several hours. This impact ionization curve tends to peak in the early morning because the electron density is lower. Therefore, the dominating energy losses are by impact ionization and excitation rather than by Coulomb collisions.

In considering Figure 6, it must be kept in mind that it refers to a location whose conjugate point has a 9° lower geographic latitude, so that the conjugate photoelectrons emanate from a region with comparatively high photoelectron production.

Over North America, the conjugate region has a higher geographic latitude, so that the conjugate impact ionization should be less important there than over Europe.

8. DISCUSSION OF THE MODEL

An important limitation to the quantitative results of this model calculation is the neutral atmosphere model (HARRIS and PRIESTER, 1962). This model is based principally on theoretical considerations and also does not allow for seasonal and latitudinal variations. Better neutral atmosphere models based on experimental data, when available, should yield better quantitative results.

The method used to calculate the escaping photoelectron flux spectrum (NISBET, 1968) seems to give reasonable agreement with observed fluxes. However, since some assumptions about this method were rather ad hoc, two other techniques have been recently proposed. BANKS and NAGY (1969) have solved a set of transport equations for upgoing and downgoing fluxes at one ionosphere. By a numerical solution in a multicomponent atmosphere for 28 eV, they calculate a daytime escape flux of 1 to 2 x 10^{11} electrons m^{-2} sec^{-1}. As seen from Figure 2 (at 27 eV for the same He II 304 Å ionization of O), the escaping flux values range from 7.5 x 10^{10} electrons $m^{-2}sec^{-1}$ at winter noon to 1.5 x 10^{11} electrons m^{2} sec^{-1} at summer noon. Taking a different approach CICERONE and BOWHILL (1969) have used

a Monte Carlo technique to simulate photoelectron diffusion through the atmosphere. Probabilities for escape at 1000 km from an initial altitude have been calculated for up to 20 eV, but the escape flux has not yet been evaluated.

In computing the impact ionization magnitude due to conjugate photoelectrons it has been assumed that the arriving flux incident at 600 km becomes entirely thermalized in the local ionosphere. BANKS and NAGY (1969), however, take into account a backscatter factor of these downgoing photoelectrons by elastic collisions with atomic oxygen. For a 28 eV photoelectron incident on a dark local ionosphere 50% are backscattered. The fraction backscattered decreases with increasing energy. Such upward fluxes from pre dawn ionospheric regions have been observed. Consequently, further evaluation of this backscatter factor for the entire photoelectron flux spectrum may decrease the resulting impact ionization (Figures 5 and 6) up to a factor of two. A somewhat compensating assumption is that a single step ionization process has been assumed. The impact ionization values shown in Figures 5 and 6 may be increased if multiple step ionization (ionization of excited atoms) is important.

The importance of these various techniques and factors can be evaluated for inclusion in further calculations with the development of improved neutral atmosphere models, the measurements of photoelectron characteristics and more detailed studies of the ionospheric electron density variations.

9. DISCUSSION OF THE RESULTS AND CONCLUSIONS

From the results plotted in Figures 5 and 6, the following conclusions can be drawn about the impact ionization due to conjugate photoelectrons:

a) During summer daytime the height integrated conjugate impact ionization represents a small (3.2% at noon) addition to the local ionization. The peak of this addition ionization rate profile (4.7% of the local) occurs above the local ionization peak (by 30 km).

b) During winter daytime the height integrated conjugate impact ionization represents a very signficiant (48% at noon) addition to the local ionization. The peak of this additional ionization rate profile (83% of the local) occurs below the local ionization peak (by 40 km).

c) During winter nighttime when the local ionosphere is not illuminated, the conjugate photoelectron impact ionization is still quite significant (0200 - 0600 hours for the geographic position studied).

In order to quantitatively ascertain the contribution of this additional impact ionization to the electron density the time dependent continuity equation would have to be solved for each altitude. The

solution of this equation is sensitive to the assumed models and reaction rates (cf. FRITZ and YEH, 1968). It does not seem realistic to carry out such a calculation now with the present uncertainties in reaction rates and the lack of sufficient data on the neutral atmosphere. However, from the results of the calculations in this paper, several qualitative conjectures can be made.

The magnitude of the height integrated impact ionization certainly is not sufficient to produce the forenoon peaks in the summer total electron content reported by LISZKA (1967). These forenoon peaks may be explained by neutral air wind effects discussed by KOHL, KING and ECCLES (1968 and 1969). However, the magnitude of the impact ionization seems sufficient to have an effect on these curves. Because of the character of the geomagnetic field with respect to geographic coordinates, each geographic location will have a unique conjugate contribution in magnitude and local time which should be observed from the total electron content measurements.

A long standing problem in ionospheric physics is the seasonal anomaly in the F2-layer critical frequency. At high latitudes there is an annual variation with the maximum in the winter. At low latitudes, the variation becomes semiannual with the maxima near the equinoxes (KING and SMITH, 1968). Comparing the magnitudes of the locally produced secondary ionization and of the conjugate ionization

with season, qualitatively, it would seem that this additional ionization gives a non-negligible contribution to these seasonal differences. The high latitude annual variation might be explained by the much larger additional ionization in winter. At low latitudes, the path losses would become negligible and the locally produced plus conjugate ionization may be a maximum at the equinoxes.

Figure 6 shows that the conjugate ionization source must be important during winter nighttime. This conjugate source could maintain the nighttime ionosphere for some hours, and even cause enhancements. Over Europe the ionization would be important in the hours after midnight because of the conjugate time difference. Over North America for instance, it would be important in the hours before local midnight. A comparison between the observations in Europe and those made at Stanford and at Hawaii by GARRIOT et al. (1965) seems to corroborate this point, although other effects certainly may be important.

An attractive feature of this additional ionization source is that it contributes at all latitudes and longitudes for which the conjugate ionosphere is illuminated above 100 km (but only within the latitudes for which the field lines are closed and for which the electric fields along the field lines are negligible).

This paper has shown that conjugate photoelectrons can be a source of ionization through impact in the local atmosphere. The

magnitude of this ionization is rather small in summer and quite significant in winter. Further model calculations and experimental observations are needed to ascertain its effect on the electron density profile and on the total electron content.

ACKNOWLEDGEMENTS

The authors wish to thank Drs. L. Liszka, H. Rishbeth, J. Nisbet, P. Banks, and T. Yonezawa for correspondence and discussions concerning this work. This work was carried out at the Royal Institute of Technology, Stockholm, and at the University of Iowa under NASA grants NGL-001-002 and NGR-16-001-043.

REFERENCES

BOSTRÖM, R. 1964 J. Geophys. Res., 69, 4983.

BROADFOOT, A. L., and HUNTEN D. M. 1966 Planet. Space Sci., 14, 1303-1319.

BUTLER, S. T., and BUCKINGHAM, M. J. 1962 Phys. Rev., 126, 1.

CARLSON, H. C., 1966 Electron Density Profiles in Ionosphere and Exosphere. (edited by J. FRIHAGEN) p. 478, North Holland, Amsterdam.

CUMMACK, C. H. 1968 J. Atmosph. Terr. Phys. 30, 125.

DUBOIN, M. L., LEJEUNE, G., PETIT, M., and WEILL, G. 1968 J. Atmosph. Terr. Phys. 30, 299.

EVANS, J. V. 1968 J. Geophys. Res. 73, 3489.

FONTHEIM, E. G., BEUTLER, A. E., and NAGY, A. G. 1968 Ann. Geophys. 24, 489.

GALPERIN, Y. I., and MULYARCHIK, T. M. 1967 Application Satellites (M. Kunc, editor), Dunod Editeur, Paris, 179.

GARRIOT, O. K., SMITH, F. L., and YUEN, P. C. 1965 Planet. Space Sci., 13, 829.

HANSON, W. B. 1963 Space Research III, Proc. Third Int. Space Sci. Symp. Washington, D. C., May, 1962, p. 282, North Holland, Amsterdam.

HINTEREGGER, H. E., HALL, L. A. and SCHMIDTKE, G. 1965 Space Res. 5, 1175.

KING, J. W. and SMITH, P. A. 1968 J. Atmosph. Terr. Phys., 30, 1707.

KOHL, H. 1966 Electron Density Profiles in Ionosphere and Exosphere (edited by J. FRIHAGEN), p. 231, North Holland, Amsterdam.

KOHL, H., KING, J. W. and ECCLES, D. 1968 J. Atmosph. Terr. Phys., 30, 1733.

KOHL, H., KING, J. W. and ECCLES, D. 1969 J. Atmosph. Terr. Phys., 31, 1011.

LISZKA, L. 1967 J. Atmosph. Terr. Phys., 29, 1243.

LOTZ, W. 1968 Z. Phys., 216, 241.

McDANIEL, E. W. 1964 Collision Phenomena in Ionized Gases, John Wiley and Sons, New York.

NAGY, A. F., FONTHEIM, E. G., STOLANSKI, R. S. and BEUTLER, A. E. 1969 J. Geophys. Res., 74, 4667-4676.

NISBET, J. S. 1968 J. Atmosph. Terr. Phys., 30, 1257.

RAO, B. C. N. and DONLEY, J. L. 1969 J. Geophys. Res., 74, 1715.

RISHBETH, H. 1968 Rev. Geophys., 6, 33.

SWIDER, W. 1965 J. Geophys. Res., 70, 4859.

THOMAS, G. R. 1968 J. Atmosph. Terr. Phys., 30, 1429.

TOHMATSU, T., OGAWA, T., and TSURUTA, H. 1965 Rep. Ionosph. Space Res. Japan 19, 482.

WATKINS, C. D. and TAYLOR, G. N. 1969 J. Atmosph. Terr. Phys., 31, 339.

WHITTEN, R. C., and POPPOFF, I. G. 1965 Physics of the Lower Ionosphere, Prentice-Hall, Englewood, Cliffs, N. J.

YOSHIZAKI, W. 1965 Rep. Ionosph. Space Res. Japan 19, 355.

Reference is also made to the following material not published in the regular international scientific literature:

BANKS, P. H. and NAGY, A. F. 1969 Paper SPA44, 1969 Fall AGU Meeting, San Francisco, and preprint submitted to J. Geophys. Res., 75.

CICERONE, R. J. and BOWHILL, S. A. 1969 Paper SPA44, 1969 Fall AGU Meeting, San Francisco and to be published Radio Sci., 5.

FRITZ, J. H. and YEH, K. C. 1968 Elect. Eng. Res. Lab., Univ. Illinois Sci. Rpt., 1.

HARRIS, I. and PRIESTER, W. 1962 Goddard Space Flight Center X-640-62-70.

FIGURE CAPTIONS

Figure 1. Primary photoelectron production rate spectrum for summer and winter noon at the conjugate hemisphere. Note that these curves exhibit broad maxima between 40 and 60 eV but that the spectrum falls off sharply above 60 eV.

Figure 2. Total conjugate escaping and local arriving photoelectron flux spectra for summer and winter local noon at 600 km altitude.

Figure 3. Total conjugate escaping and local arriving photoelectron flux as a function of conjugate and local time, respectively, for summer and winter.

Figure 4. Comparison of calculated and observed photoelectron flux values ($E > 5$ eV) near sunrise and sunset. The observed values are from RAO and DONLEY (1969). At solar zenith angles of 86.4° and 91.9° calculated flux values are given for both sunrise and sunset, the sunrise value being higher as expected.

Figure 5. Impact ionization rate profiles due to conjugate photoelectrons for local summer and winter noons. The local photo plus secondary ionization and the loss probability are plotted for comparison.

Figure 6. Height integrated conjugate photoelectron impact ionization rate for summer and winter local daytimes. The times of local sunrise (LSR), local sunset (LSS) and conjugate noon (CN) are indicated by arrows. For comparison, the height integrated photo plus secondary ionization rate is also shown.

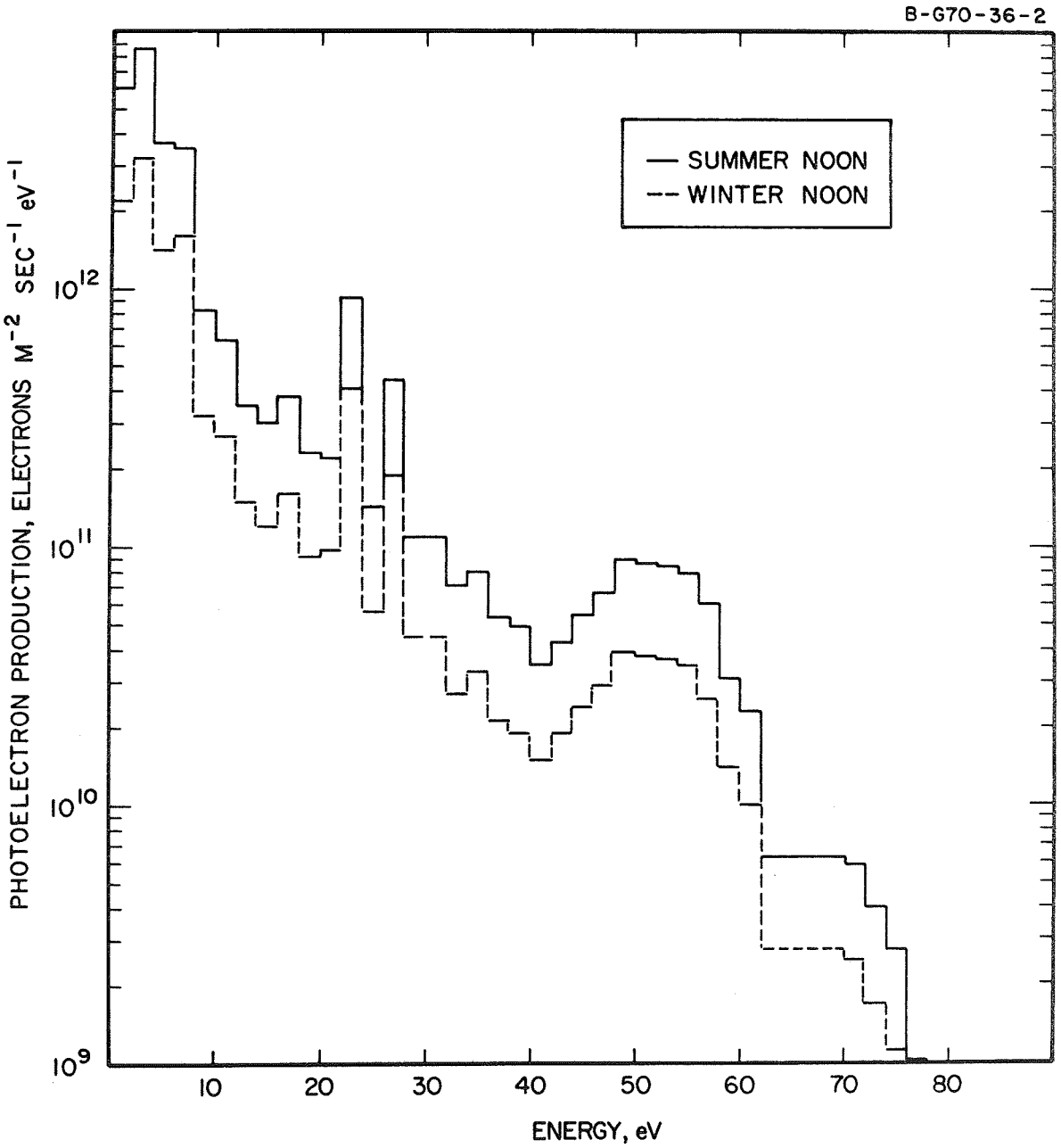
B-G70-36-2
— SUMMER NOON
-- WINTER NOON
PHOTOELECTRON PRODUCTION, ELECTRONS M^{-2} SEC^{-1} eV^{-1}
10^{12}
10^{11}
10^{10}
10^{9}
10
20
30
40
50
60
70
80
ENERGY, eV

Figure 1

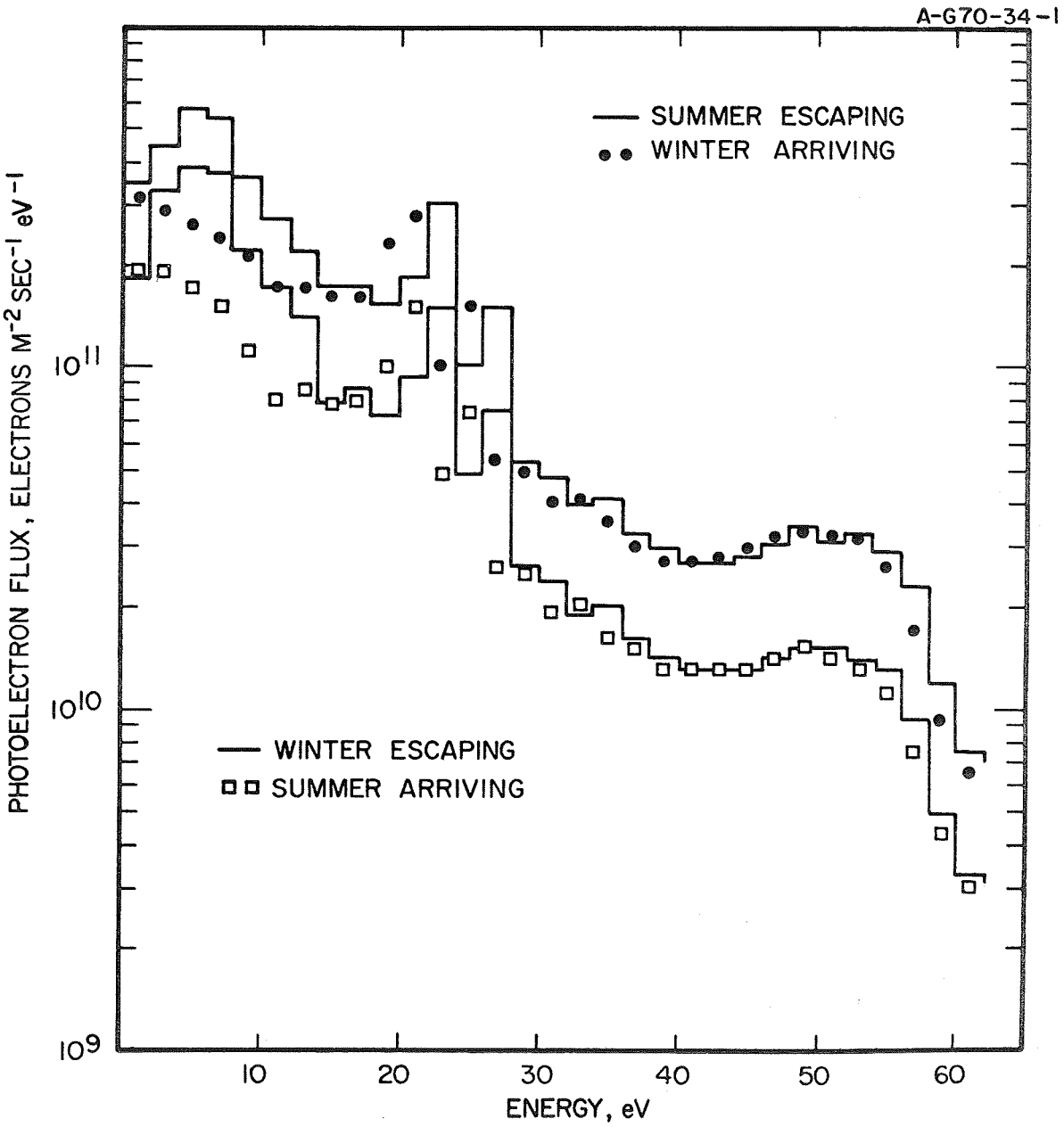
A-G70-34-1
SUMMER ESCAPING
WINTER ARRIVING
WINTER ESCAPING
SUMMER ARRIVING
PHOTOELECTRON FLUX, ELECTRONS M-2 SEC-1 eV-1
10^11
10^10
10^9
10
20
30
40
50
60
ENERGY, eV

Figure 2

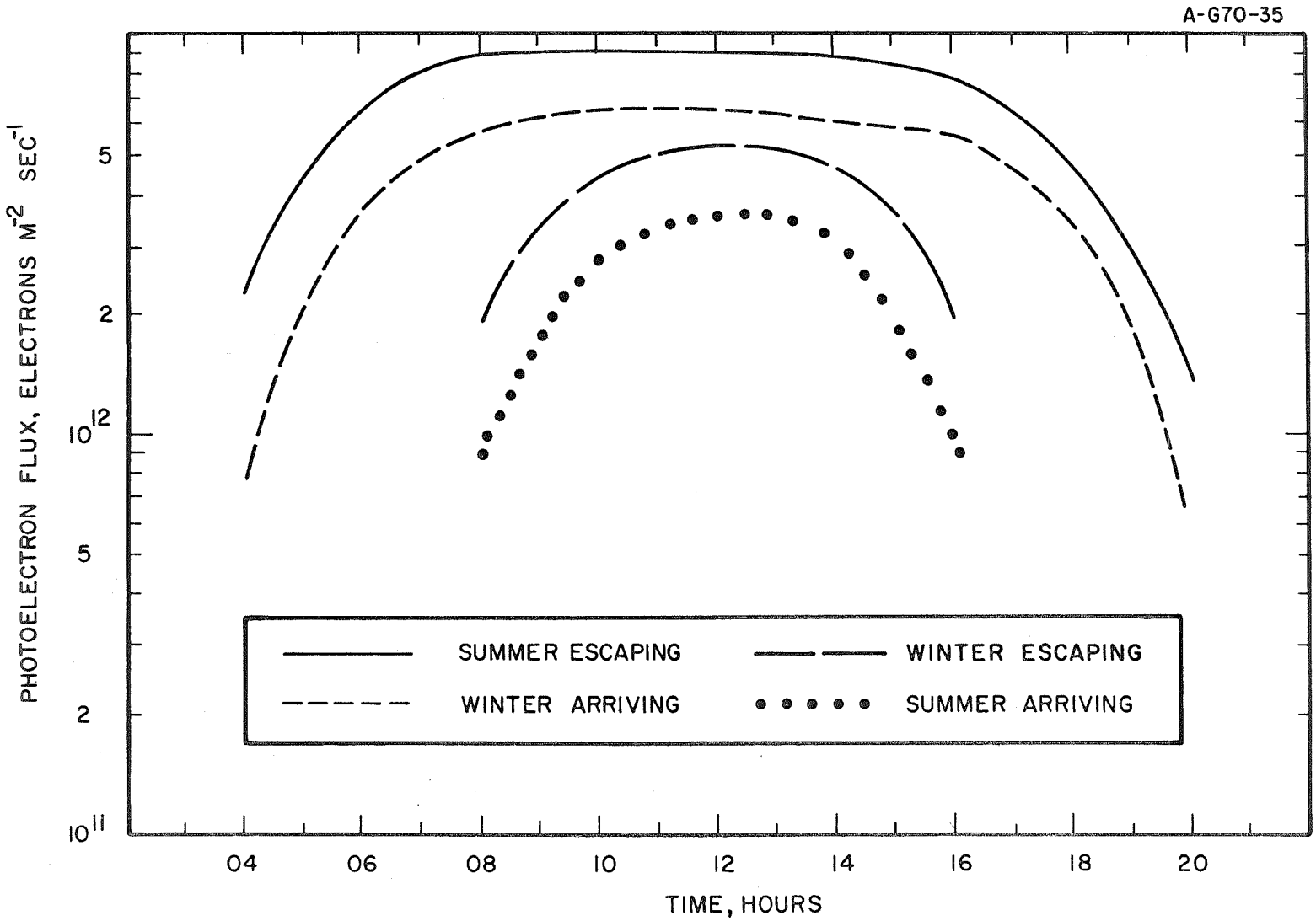
A-G70-35
PHOTOELECTRON FLUX, ELECTRONS M^{-2} SEC^{-1}
5
2
10^{12}
5
2
10^{11}
04
06
08
10
12
14
16
18
20
TIME, HOURS
SUMMER ESCAPING
WINTER ESCAPING
WINTER ARRIVING
SUMMER ARRIVING

Figure 3

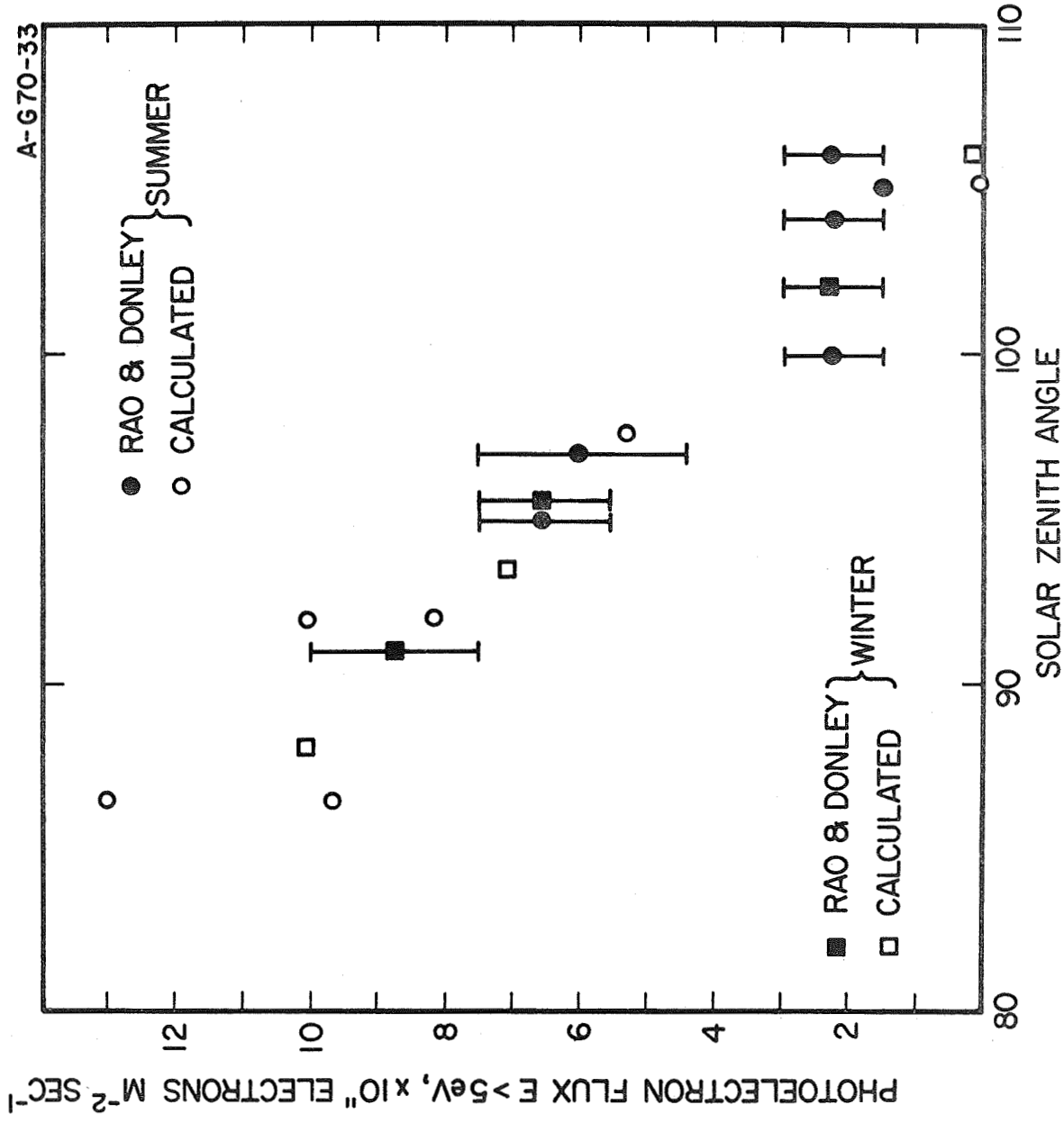
A-G70-33
RAO & DONLEY
CALCULATED
SUMMER
RAO & DONLEY
CALCULATED
WINTER
PHOTOELECTRON FLUX E >5eV, x10" ELECTRONS M-2 SEC-1
SOLAR ZENITH ANGLE
2
4
6
8
10
12
80
90
100
110

Figure 4

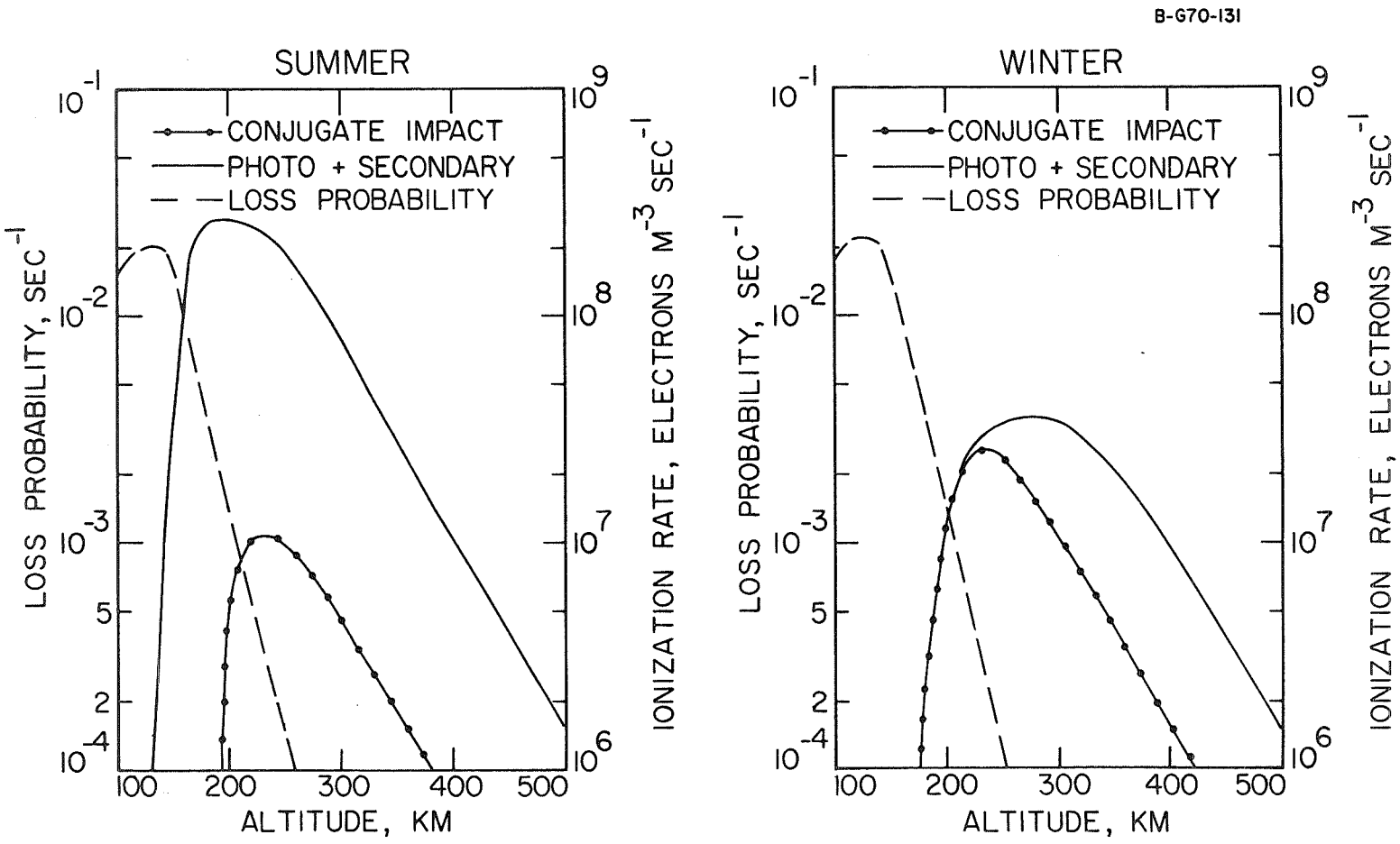
B-G70-131
SUMMER
WINTER
CONJUGATE IMPACT
PHOTO + SECONDARY
LOSS PROBABILITY
LOSS PROBABILITY, SEC^{-1}
IONIZATION RATE, ELECTRONS M^{-3} SEC^{-1}
ALTITUDE, KM
10^{-1}
10^{-2}
10^{-3}
5
2
10^{-4}
10^{9}
10^{8}
10^{7}
10^{6}
100
200
300
400
500

Figure 5

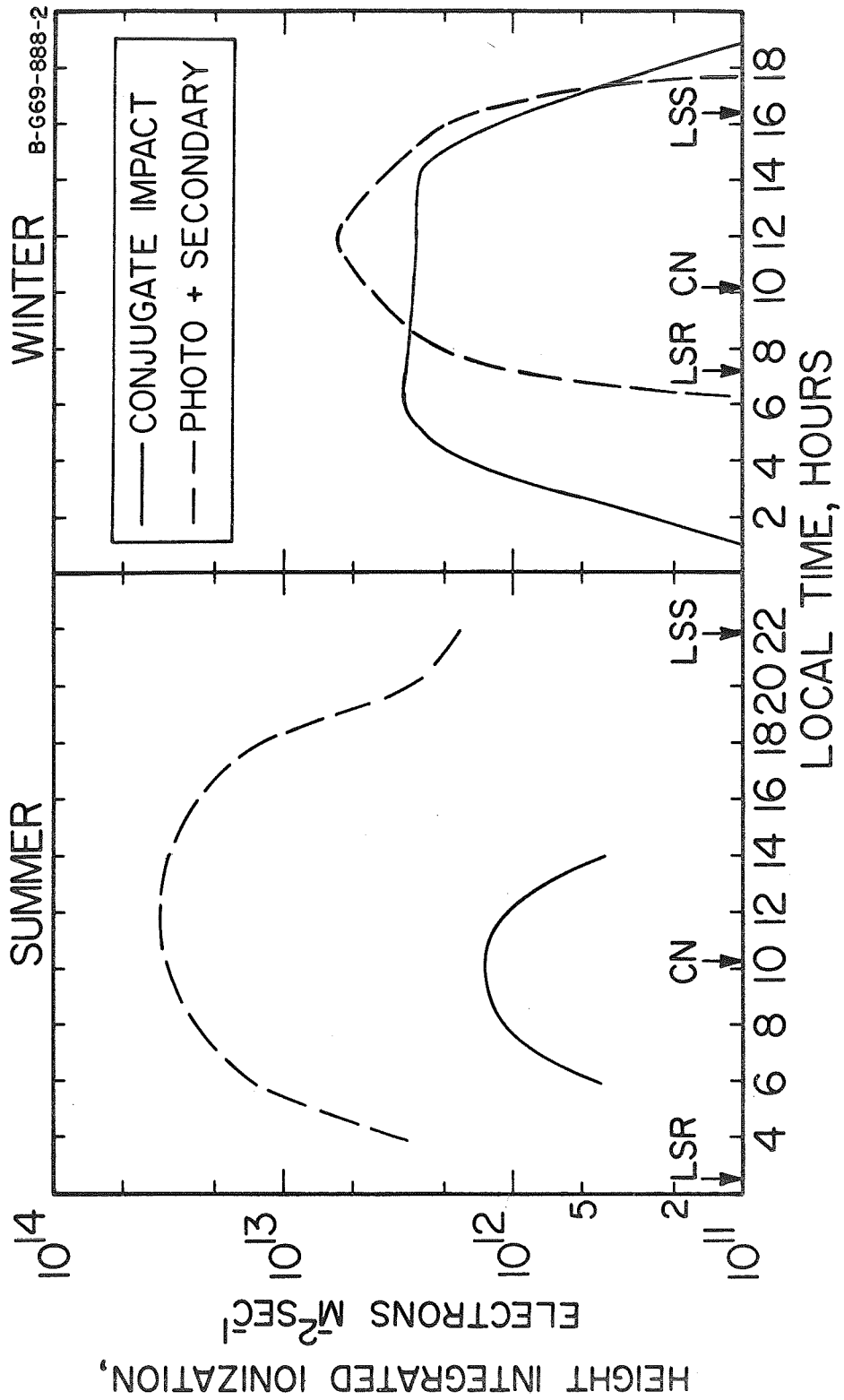
B-G69-888-2
SUMMER
WINTER
CONJUGATE IMPACT
PHOTO + SECONDARY
LSR
CN
LSS
LSR
CN
LSS
4 6 8 10 12 14 16 18 20 22
2 4 6 8 10 12 14 16 18
LOCAL TIME, HOURS
10^{14}
10^{13}
10^{12}
5
2
10^{11}
HEIGHT INTEGRATED IONIZATION, ELECTRONS $M^{-2}SEC^{-1}$

Figure 6